Superconducting tunneling into the $A15$ Nb_3Al thin films

J. Kwo and T. H. Geballe*
Department of Applied Physics, Stanford University, Stanford, California 94305
(Received 1 October 1980)

Single-particle (Giaever) tunneling has been performed on $A15$ Nb_3Al thin films with good-quality junctions formed by oxidized amorphous-silicon barriers. The tunneling measurement is used as a diagnostic probe for assessing the material properties of Nb_3Al, including changes in the progressive film growth. The electron-phonon spectral function $\alpha^2F(\omega)$ and related physical parameters are generated by the proximity-effect inversion analysis of the tunneling density of states. We find that Nb_3Al is a strong-coupled superconductor with $2\Delta/k_BT_c \geq 4.4$ only when the composition approaches the $A15$ phase boundary (24 at.% Al). A difference in the low-frequency behavior of $\alpha^2F(\omega)$, observed between two junctions of different coupling strength, strongly suggests the importance of a mode softening mechanism, and implies that the average $\langle\omega\rangle$'s are rather sensitive to composition, or perhaps disorder. The lattice of Nb_3Al being softer than Nb_3Sn and V_3Si contributes significantly to the large λ and the high T_c of Nb_3Al.

I. INTRODUCTION

The high-transition-temperature $A15$ superconductors are of continuing interest in terms of both their basic properties and their technological applications. The two canonical $A15$ compounds V_3Si can be grown as stoichiometric and ordered single crystals from which well-characterized samples can be obtained. Numerous physical measurements and theoretical model calculations have advanced the understanding a great deal in the past. It is generally agreed that the existence of a high density of states with a sharp peak near the Fermi level plays an essential role in the high-T_c superconductivity and some normal-state properties.[1] Electron tunneling into all the $A15$'s, the most direct probe of the microscopic superconductivity, however, has been difficult for two reasons. First, the native oxides of many transitional metals and compounds usually do not form good insulating tunnel barriers and lead to poor tunnel characteristics. Second, the very short coherence length of the $A15$ compounds requires maintaining the proper superconducting structure within a few atomic layers of the surface in order to obtain good tunneling. Recently, advances in electron-beam coevaporation together with improved methods of barrier formation have made possible high-quality tunnel junctions on Nb_3Sn (Refs. 2 and 3) and V_3Si.[2]

Another class of $A15$ compounds, including Nb_3Al, Nb_3Ga, Nb_3Ge, and probably Nb_3Si can be prepared under some nonequilibrium conditions as the highest T_c superconductors known. The metastable character of the $A15$ phase in this class of materials demands a good understanding and control of the sample preparation method and requires the use of some unconventional synthesis techniques. Physical measurements[4,5] on the available samples in this metastable class have for some time shown results conflicting with the models used for V_3Si and Nb_3Sn, suggesting the possibility that a different source is responsible for the high T_c's.[4,6] However, the definite evidence of inhomogeneities in composition and phase which exist to varying degrees in many of these materials, as shown by the broad transitions in the heat-capacity measurements,[4,5] weakens the above assertion and leaves the issue unsettled.

Nb_3Al serves as prototypical example for the above difficulties and, as the least unstable member of this class, has the best prospect of improved understanding. Although the high T_c is achievable by bulk metallurgical techniques, the very limited temperature range over which the stoichiometric composition is approached makes the preparation of homogeneous $A15$ samples close to stoichiometry unlikely.[7] Heat-capacity[4] and magnetic susceptibility[8] measurements on bulk Nb_3Al show a low electronic density of states at the Fermi level and temperature-independent normal-state properties. In addition, the neutron scattering function $G(\omega)$ of Nb_3Al obtained from inelastic neutron scattering[9] is representative of a weak to medium coupled superconductor. Therefore it appears difficult, within the conventional framework of superconductive theory, to attribute the high T_c superconductivity of Nb_3Al to the same cause as V_3Si or Nb_3Sn.

As an initial step in resolving the above controversy and understanding better the mechanism giving rise to the high T_c's in the metastable $A15$'s, we have undertaken a comprehensive study of the properties of Nb_3Al. An investigation of the $A15$ phase equiliriums and conditions for preparing homogeneous thin films was first carried out and described in Ref.

10. In the present work, we have studied the single-particle (Giaever) tunneling into these well-characterized Nb_3Al thin films and obtained microscopic parameters of superconductivity, including λ, μ^*, and $\langle\omega\rangle$'s. Based on our results, we discuss the important implications and suggest an interpretation not based on a high density of states near the Fermi level to describe the high T_c superconductivity in A15 Nb_3Al.

II. EXPERIMENTAL PROCEDURES

The Nb_3Al thin films were prepared by the electron-beam coevaporation technique of Hammond,[11] in which the chemical composition and deposition parameters can be well controlled. The optimum deposition conditions found in the earlier synthesis work[10] are at substrate temperatures from 950 to 1050 °C and deposition rates from 15 to 30 Å/sec. The total film thickness is typically about 5000 Å. Sapphire substrates of $\frac{1}{4}$-in. square were arranged in the geometry with the row major axis either parallel or perpendicular with respect to the line connecting the Nb and Al sources. The former configuration generates a compositional spread across a series of substrates and the latter provides many samples of nearly constant compositions.

For tunnel junction formation, the Nb_3Al films were cooled from the high-deposition temperatures to below 100 °C within 20 min. Initially the barrier used was the oxide mixture of Nb_3Al formed by the thermal oxidation in room air ambient for a few hours. In later runs, oxidized amorphous-silicon barriers were employed, because they were recently shown to be successful on the transition-metal compounds V_3Si (Refs. 2 and 12) and Nb_3Sn.[2,3] Before breaking the vacuum to atmosphere, a thin layer of amorphous silicon was deposited onto the Nb-Al film surface at a rate of 1.5 Å/sec and at a substrate temperature $\leq$100 °C. The sample surfaces were then oxidized in the room air about 3–5 h. Finally, the junctions were defined by hand painting a thin insulating layer of polysterene Q dope, and completed by evaporating Pb counterelectrodes.

III. RESULTS

A. Tunneling barrier properties

The first essential task in a tunneling experiment is to form a reliable, insulating barrier. The Nb_3Al oxide mixture forms a medium-quality barrier by itself, exhibiting better tunneling characteristics than those of Nb_3Sn (Ref. 3) and V_3Si.[2] A 1–2-h thermal oxidation gives a junction resistance as high as 90–130 Ω. As shown by the top *IV* curve in Fig. 1,

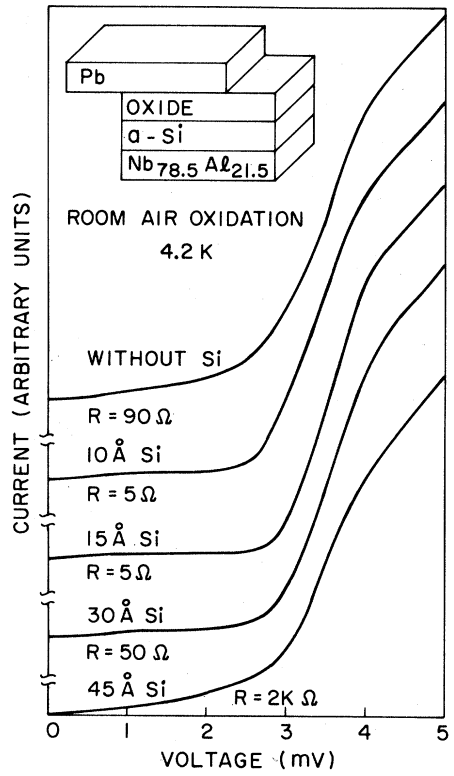

FIG. 1. Current-voltage characteristics at 4.2 K of A15 Nb-Al (of 21.5 at.% Al) tunnel junctions with the thickness of the *a*-Si overlay varying from 0 to 45 Å.

the conduction at voltages below the sum gap is rather substantial, resembling the characteristics of thermally oxidized Nb junctions.[13,14]

Employing a thin Si barrier about 10–20 Å effectively cuts down the excess conduction below the sum gap to less than 5% and reduces the junction resistance to about 1–5 Ω, as illustrated by the 2nd and 3rd curves in the same figure. Thicker Si overlays of 30 Å or more result in less satisfactory tunneling characteristics and an exponential increase of the junction resistance. In addition, a significant curvature appears in the *IV* curve at high bias. The deviation from the expected linear behavior is presumably caused by unoxidized silicon which makes a more complicated barrier.

Based on these observations of the distinct tunnel characteristics for junctions made with and without a thin Si overlay and of the exponential increase of the junction resistance with Si thickness, it is inferred that the tunneling is essentially through the oxidized silicon barrier. Pinholes, if any exist, are blocked by the very resistive native oxide of Nb-Al, and do not contribute to the conduction substantially. This result is in good agreement with a proposed model by Rudman and Beasley[15] to describe the detailed properties of oxidized amorphous-silicon barriers.

Furthermore, we find that Si barriers of 10–20 Å yield good-quality tunnel junctions routinely, and relatively independently of the oxidation procedure. The junction resistance increases only slightly with the increased humidity during oxidation. In contrast, the oxide mixture of Nb_3Al fails by oxidation in an acetic acid atmosphere, which was shown to be favorable for oxidizing In (Ref. 16) and Nb_3Sn.[3] The robust and reliable reliable features of the Si barrier permits using tunneling as a material diagnostic tool, as described in Sec. III B.

Under similar deposition conditions used in preparing the silicon barriers, thin Al overlays of 10–25 Å were tried as tunnel barriers and were not successful. The excess conduction below the sum gap is not reduced, even with a rather large increase of junction resistance into the kΩ range. Since a thin Al overlay deposited near room temperature rarely yields a uniform coverage, the pinholes are filled up by the less resistive native oxide of Nb-Al. Tunneling is then essentially through the Nb-Al oxide, leading to undesired tunnel characteristics. Our results suggest that an Al barrier could not be satisfactorily formed free of pinholes without resorting to a thicker overlay $\gtrsim$60 Å or using some special oxidation process.[17]

B. Tunnel characteristics versus composition

It was found in Ref. 10 that depositions at the optimum substrate temperatures (~950–1050 °C) yield as ordered an *A*15 structure as allowed by the composition. In the single phase *A*15 region (~17–21.5 at.% Al), the transition temperatures (T_c's) are then essentially a linear function of the Al composition. Figure 2 shows the representative *IV* curves for a series of Nb-Al–oxidized *a*-Si–Pb junctions from one deposition at 950 °C in the composition-spread configuration. In the single phase *A*15 region, the energy gaps are found to increase monotonically with the Al composition. Defining the sum gap ($\Delta_{Nb-Al}+\Delta_{Pb}$) to be the voltage at the inflection point of the rise of the gap, a maximum value of 3.5 meV near the phase boundary of 21.8 at.% Al is reached. Since the coherence length of the *A*15 Nb_3Al is only about 30 Å, there is a question as to whether the superconducting properties exhibited by the material near the surface, which the tunneling probes, are representative of those of the entire sample. A useful check is to compare the inductively measured transition temperature T_c^L of the entire sample with the surface energy gap Δ, since deteriorated superconductivity at the surface will give values of $2\Delta/k_BT_c$ less than the BCS value 3.53. Values close to 3.5–3.6 are obtained for most Nb-Al tunnel junctions except for the very Nb-rich samples which exhibit a larger scattering in the T_c^L values. The satisfactory correlation between the energy gaps measured near the surfaces and the bulk T_c's suggests that homogeneous growth over the total film thickness has been achieved in most samples.

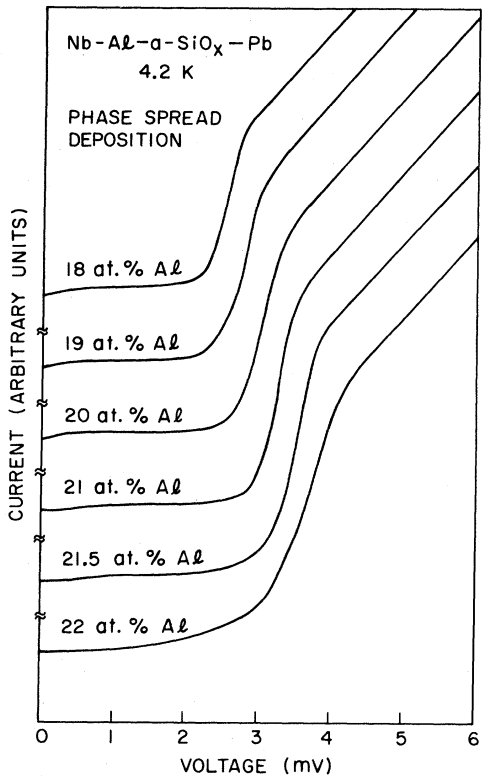

FIG. 2. Current voltage characteristics at 4.2 K of a series of *A*15 Nb-Al junctions obtained from a phase-spread deposition at 950 °C. The thickness of the *a*-Si overlay is of 15 Å. The *A*15 phase boundary is at 21.8 at.% Al.

For junctions of the single phase *A*15, the leakage as measured by zero-bias conductance is indeed quite small, about 10^{-3} of the normal-state conductance, indicating that a good-quality tunnel barrier is formed by the oxidized amorphous silicon. However, nearly all junction characteristics commonly exhibit an excess conductance, about 2–5% of the normal-state conductance, above the Pb gap. This suggests a finite density of states inside the gap in the Nb-Al electrode, even in the very Nb-rich *A*15 samples. This normal-like material inclusion was also observed in Nb_3Sn (Refs. 2 and 3) and V_3Si,[2] yet the origin remains unclear.

For the Al composition $\gtrsim$22 at.%, the *IV* characteristic deteriorates substantially, with a large conduction below the gap. Because of the reliability of the Si barrier, we attribute such an excess conduction to an additional amount of a normal phase in the Nb-Al electrode. This is consistent with the x-ray-diffraction analysis which shows an increasing concentration of the second phase Nb_2Al.

The width of the gap increases toward the higher-energy direction for junctions in the two phase re-

gion. In some cases a second gap about 0.3 meV higher can be resolved. A corresponding behavior of the transition temperature is also observed; the maximum T_c for a given phase-spread deposition occurs in the samples which contain a slight amount of second phase.

The very small zero-bias conductance is still maintained for junctions where the second phase is present. This is consistent with the observation that the film texture remains the same indicating no dramatic change in the surface morphology and thus continued good tunnel barrier formation.

C. Tunneling and self-epitaxial growth

Recently Dayem *et al.*[18] have shown that the metastable *A*15 phase becomes more energetically favored in an epitaxial growth by interfacing with an underlying ordered *A*15 substrate of a close lattice-constant match. Such a stabilization method results in suppressing the unwanted second-phase growth and therefore extending the *A*15 phase boundary. In case of the self-epitaxial deposition reported previously,[10] this involves depositing nearly stoichiometric Nb_3Al films, which by themselves would be of two phase, on top of the single phase *A*15 Nb-Al films of only 20 at.% Al. The beneficial results are extending the *A*15 phase boundary to 1 at.% Al higher with a T_c enhancement about 2 K. The initial tunneling results showed unexpectedly that the energy-gap values of the epitaxial samples, which were grown as bilayers of 0.5 μm each, were no different from those of the samples made without the self-epitaxial deposition. Since overall T_c^L's of the epigrown samples are enhanced by more than 2 K, the superconductivity exhibited by the surface material appears to be depressed. This situation is in contrast with the previous finding that a homogeneous growth can be achieved in a conventional deposition.

To resolve this puzzle, we have carried out tunneling measurements on a series of self-epi-grown samples, of the same composition, but with a varying epilayer thickness. Since the tunneling experiment probes the material only within a few coherence lengths of the surface, any inhomogeneity in the growth will manifest itself through the changes in the IV characteristics with varying epilayer thickness. The experiment was done by carrying out the self-epitaxial deposition in the constant-composition direction as shown in Fig. 3. The chemical composition is maintained nearly constant across the 10 substrates of each row (*A*) or (*B*), while there is a compositional difference of about 1 at.% Al between (*A*) and (*B*) rows. By maneuvering the shutter during the epilayer deposition, a gradual change in epilayer thickness was generated across the 10 samples of each row. The tunnel junctions were then formed on these film surfaces by the normal procedures.

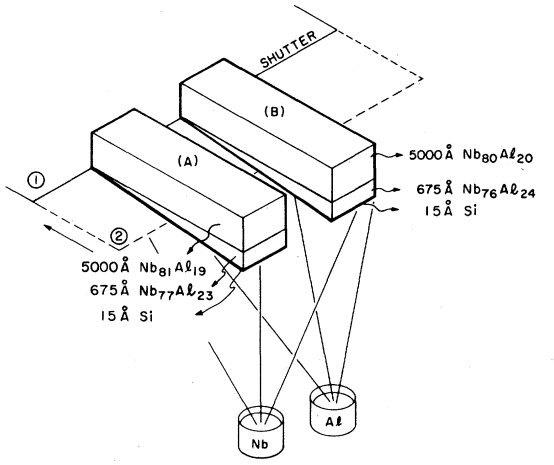

FIG. 3. Configuration for the self-epitaxy deposition in the constant phase direction at 950 °C. The epitaxial layer thickness is varying from zero at one end of the 10 substrates to 675 Å at the other end.

Figure 4(a) shows the *IV* curves obtained as a function of the epilayer thickness *d* for (*A*)-row samples from one run at 950 °C. For *d* less than 45 Å, the junction characteristics (not shown) are more complicated, probably as a result of the uneven film coverage during the initial stage of the epilayer deposition. As *d* increases from 45 up to 90 Å, the value of the sum gap progressively increases from 2.5 meV of the underlying substrates and reaches the full value of 3.5 meV normally obtained in a deposition without self-epitaxy. However, the energy gap continuously rises above 3.5 meV as *d* is increased above 90 Å. Note that the excess conductance below the gap is rather small. In addition, the spread in the gaps becomes narrower. A maximum value of the sum gap of 4.0 meV is reached at an epilayer thickness 150 Å. Further increase of the epilayer thickness above 150 Å results in a gradual decrease of the gap and an appearance of the "proximity knee" just above the rise of the gap, suggesting that the surface progressively degrades from the underlying material.[19] Finally, the gap value stays constant as low as 3.5 meV for *d* at and greater than 480 Å. It is clear that an improved growth over only a finite thickness less than 200 Å can be sustained from a self-epitaxial interface. Since the inductive T_c measurement senses only the highest-T_c layer of the entire sample, a correct description of the overall material growth is often obscured.

For the adjacent row-(*B*) samples of higher Al composition, similar systematics of *IV* curve versus epilayer thickness were also observed, as shown in Fig. 4(b). The maximum enhanced gap, of 4.5 meV

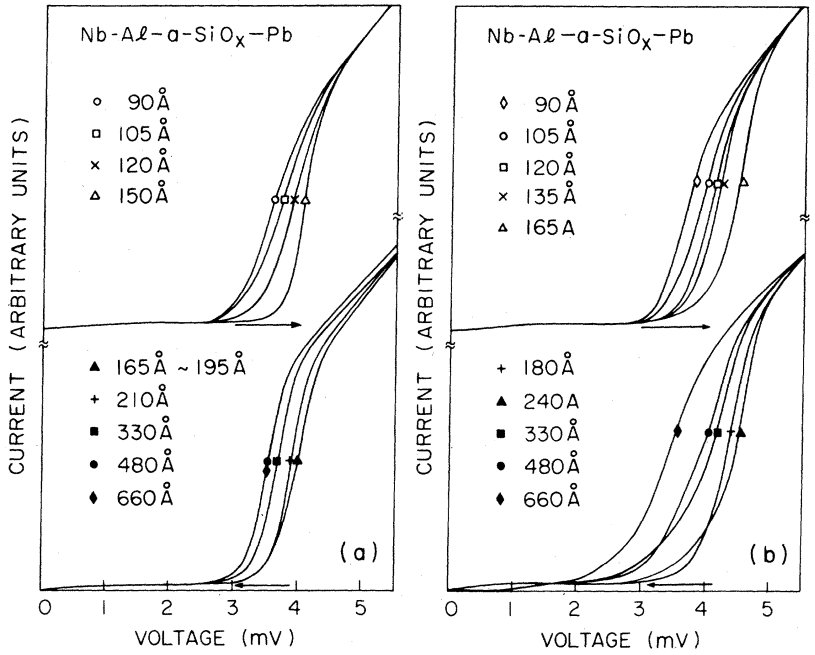

FIG. 4. (a) Current vs voltage at 4.2 K of a series of tunnel junctions on the (*A*)-row self-epitaxial samples with epilayer thickness *d* systematically increasing from 90 to 660 Å. The composition of the epilayer is of 23 at.% Al. (b) The same for the (*B*)-row self-epitaxial sample. The composition of the epilayer is of 24 at.% Al.

for the sum gap, occurs at an epilayer thickness of 165 Å. Thicker epilayer depositions yield a decrease of the gap value and an increase of the excess conduction below the gap, due to the emerging growth of the normal phase Nb_2Al. For *d* at 660 Å and greater, the tunnel chracteristics are the same as those of a two-phase composition obtained in a normal deposition without epitaxy.

Based on the above results, one can attribute the enhanced energy gaps and T_c's to an improved film growth stabilized by an underlying *A*15 substrate. For thicker films this enhanced growth eventually degrades and the structure relaxes back to that obtained in a normal deposition. The possibility of a proximity effect from the underlying lower-T_c substrates has been estimated. In fact, such effect may account for the systematic increase of the gap value from that of the underlying substrates with the epilayer thickness up to 165 Å. The resultant depression in the measured T_c^{max} is estimated to be about 1 K.

D. Coupling strength versus composition

Collecting all tunneling data obtained from depositions with and without self-epitaxy, we plot in Fig. 5 the electron-phonon coupling strength $2\Delta/k_BT_c$, as a function of the Al composition up to 22.8 at.%. The data cover T_c's ranging from 9.4 to 16.4 K and energy gaps (Δ's) varying from 1.15 up to 3.15 meV. The error bars are determined by the widths of the T_c's and the gaps. The Al composition is corrected to be only of the *A*15 components[20]; as necessary for the slightly two-phase samples. For the data at 21.5 and 22.8 at.% Al, T_c's are determined to be the temperatures at which the gaps open. The Nb_3Sn data obtained in a similar fashion by Moore *et al.*[2] are

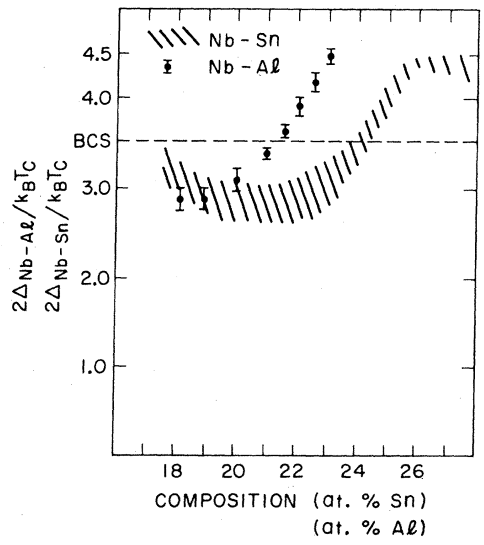

FIG. 5. The variation with composition of the coupling constant $2\Delta_{Nb-Al}/k_BT_c$ and $\Delta 2_{Nb-Sn}/k_BT_c$. The data of Nb_3Sn are after Moore *et al.* (Ref. 2).

plotted for comparison. It is found that Δ_{Nb_3Al} is more sensitive to the composition than is T_c. The $2\Delta/k_BT_c$ ratio for A15 Nb-Al remains BCS-like for the Al composition $\leq$21.5 at.%, and rises rapidly up to 4.4 at 22.8 at.% Al. Similarly, it has been found that A15 Nb_3Sn becomes strong coupled only when the composition approaches stoichiometry.

The origin of this dramatic change of the electron-phonon coupling strength of Nb_3Al with the composition approaching the A15 phase boundary is not well understood. An insight can be gained from referring to the analytical formula by Kresin *et al.*,[21]

$$2\Delta/k_BT_c = 3.53[1+5.3(T_c/\omega_0)^2\ln(\omega_0/T_c)] ,$$

which expresses the enhancement of the coupling strength $2\Delta/k_BT_c$ as an explicit function of the ratio T_c/ω_0, where ω_0 is a characteristic Einstein phonon frequency. An analysis based on this formula shows that a change in the $2\Delta/k_BT_c$ ratio from BCS-like to a value as large as 4.4 requires a substantial increase in T_c/ω_0. Since T_c varies only modestly, from 14.0 to 16.4 K, the occurrence of phonon-mode softening, i.e., a smaller ω_0, appears necessary to account for the large increase in T_c/ω_0. The most direct proof of this supposition is to examine the $\alpha^2F(\omega)$ functions obtained experimentally from tunneling densities of states, as described in Sec. III E.

E. Tunneling density of states and $\alpha^2F(\omega)$

The dynamic resistance dV/dI as a function of the bias voltage has been measured for several Nb-Al junctions of importance. Data of the superconducting state were taken at 1.5 K with a magnetic field $\sim$1 kG applied to quench the superconductivity in Pb. Throughout the data reduction, a constant excess conductance, of about 2–5% of the normal-state conductance, was subtracted out from both the superconducting and the normal-state tunneling conductance. The energy gap Δ was determined experimentally with the aid of Bermon's table.[22] The reduced tunneling density of states $R(\omega)=N_{expt}(\omega)/N_{BCS}(\omega)-1$ was then calculated. Figure 6 shows the $R(\omega)$'s for two particular junctions. One is a relatively weak coupled superconductor, with a T_c of 14.0 K and a gap of 2.15 meV; the other is strong coupled, of larger Al composition by 1.3 at.%, with a higher T_c at 16.4 K and a gap of 3.15 meV. A reduction in the magnitude of $R(\omega)$ is found as the Al composition is reduced, indicating a weakening in the electron-phonon coupling strength. However, the overall shapes of the two $R(\omega)$'s are rather similar, and there is no dramatic change in the positions of structures induced by phonons. Similar behavior is found in the tunneling densities of states of Nb_3Sn junctions of different T_c's and coupling strength.[23]

The electron-phonon spectral function $\alpha^2F(\omega)$ has been generated from the input data of $R(\omega)$ and Δ by the gap-inversion analysis for these two junctions. The initial method employed was the conventional McMillan-Rowell inversion program.[24] For the junction with a T_c of 16.4 K and a Δ of 3.15 meV, that analysis gives a value of only 0.6 for the electron-phonon interaction parameter λ and a negative value $\sim$−0.10 for the effective Coulomb pseudopotential μ^*. The calculated T_c from these parameters is thus less than 10 K. Perhaps the most unphysical result using that analysis is that a high-energy cutoff of less than 30 meV had to be imposed to prevent the iterative solutions from becoming unstable. The structure between 20 and 40 meV, as associated with the Al phonons, was then left out entirely. Furthermore, as shown in Fig. 7, there is a large positive offset between the experiment and the calculated $R(\omega)$'s.

Similar problems have also been encountered in

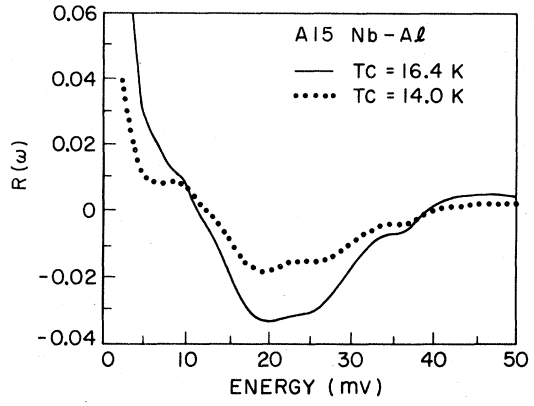

FIG. 6. Reduced tunneling density of states $R(\omega)$ vs energy above the gap for the two Nb-Al junctions of $T_c=16.4$ K, $\Delta=3.15$ meV and $T_c=14.0$ K, $\Delta=2.15$ meV, respectively.

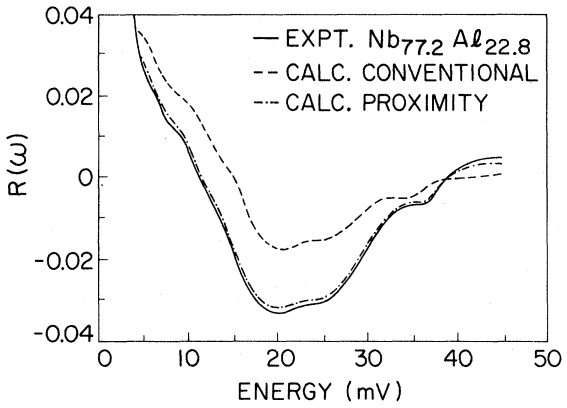

FIG. 7. The experimental and calculated tunneling densities of states $R(\omega)$'s from both conventional and proximity inversion analysis for the A15 Nb-Al junction of 22.8 at.% Al with $T_c=16.4$ K and $\Delta=3.15$ meV.

the analysis of tunnel data of other transition metals or compounds, such as thermally oxidized tunnel junctions of Nb (Ref. 14) and Nb_3Sn.[25] Recently the modified McMillan-Rowell (MMR) inversion analysis based on the model of proximity-effect tunneling, proposed by Arnold[26] and implemented by Wolf *et al.*,[27] has permitted an improved description, i.e., more self-consistent, of the tunneling data of such Nb and Nb_3Sn junctions within the conventional framework of the strong-coupling theory.[28,29] In this model a thin layer of weakened superconductivity is proposed to exist between the insulating oxide and the base electrode, and it is characterized by a constant pair potential $\Delta_n << \Delta_s$ and a thickness of $d_n << \xi$.

It is plausible that a thin proximity layer exists between the Nb_3Al film and the *a*-Si oxide barrier. It could possibly be caused by the exposure to the residual gaseous impurities in the vacuum chamber during the long period cooling from high temperature before the Si overlay is deposited, or by the disordered or compositional variation inherent in the atomic structures near the surface. The evidence of a "knee"-like structure above the rise of current at the sum-gap in the *IV* characteristic has been observed in some Nb-Al junctions. Such a structure has been attributed to a proximity layer.[26]

With no *a priori* knowledge about this promixity layer, we approximate it with $\Delta_n = 0$. The tunneling density of states is then, as shown in Ref. 26, dependent on two additional parameters, $2d_n/\hbar v_F^*$ and d_n/l, where d_n, v_F^*, and l are the thickness, the renormalized Fermi velocity, and the mean free path of the proximity layer, respectively. As shown in Fig. 7, the proximity inversion yields a satisfactory agreement, to within 2%, between the calculated and the experimental $R(\omega)$'s with properly chosen parameters of $2d_n/\hbar v_F^* \sim 0.006$ $(\text{meV})^{-1}$ and $d_n/l \sim 0.055$. The criteria used to determine these fitting parameters are based on the requirement of generating a proper cutoff at high-energy end in $\alpha^2F(\omega)$ and in reproducing the phonon-peak positions correctly. Furthermore, this analysis gives acceptable values of $\lambda = 1.7$ and $\mu^* = 0.15$, leading to a reasonable value for the calculated[30] T_c. The corresponding electron-phonon spectral function $\alpha^2F(\omega)$ is presented in Fig. 8 by the solid circles. The resulting physical parameters and the average frequency moments are summarized in Table I. Taking the calculated $\langle\omega_{\log}\rangle$ as the characteristic Einstein mode entering in the formula of Kresin *et al.*,[21] a value of 4.3 for $2\Delta/k_BT_c$ is obtained, in close agreement with the experimental value 4.4.

For the other junction with a lower T_c of 14.0 K and a smaller Δ of 2.15 meV, the proximity inversion method again provides a better description of the tunneling data. Good agreement betwen $R(\omega)_{\text{expt}}$ and $R(\omega)_{\text{calc}}$, to the same degree as for the previous

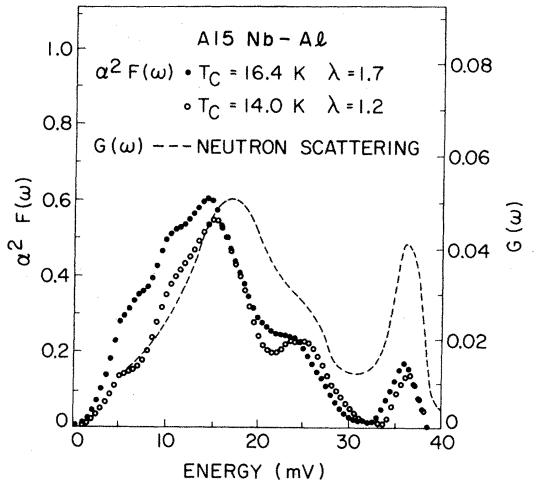

FIG. 8. The electron phonon spectral functions $\alpha^2F(\omega)$ for two Nb-Al junctions with $2\Delta/k_BT_c$ of 3.6 and 4.4. The data of the neutron scattering function $G(\omega)$ are after Schweiss *et al.* (Ref. 9).

junction, was achieved with similar values of the proximity parameters. The resulting $\alpha^2F(\omega)$ is shown in Fig. 8 by the hollow circles. The overall features of the $\alpha^2F(\omega)$ functions of these two junctions are quite similar, with a slight reduction of about 10% in the $\alpha^2F_{\max}$ for the lower-T_c one. However the strong-coupled and high-T_c junction shows a pronounced enhancement in the weightings of the low-frequency phonons, leading to smaller values of the frequency moments. In fact, the significant reduction of λ, from 1.7 to the 1.2 found for the lower-T_c junction, is mainly from the stiffening of phonons; i.e., $\langle\omega^2\rangle$ is larger by 20%. The $\alpha^2F(\omega)$ presently obtained is not completely determined by the data because of the assumed ω^2 dependence at $\omega \lesssim 5$ meV. Nevertheless, such parabolic fit at small ω does not affect in any sensitive way the quantitative results of λ, μ^*, $\langle\omega\rangle$'s, and the correlation of the enhanced low-frequency weightings in $\alpha^2F(\omega)$ with strong coupling. Thus our analysis of the tunneling data strongly supports the mode softening mechanism previously supposed.

In the same figure, we also show the neutron scattering function $G(\omega)$ from the work of Schweiss *et al.*[9] Agreement with the cutoff energy and the structures at about 16, 25, and 36 meV, associated with the Nb and the Al phonons, respectively, is quite acceptable. However, a large discrepancy does occur in the low-frequency portion of the spectrum, particularly between $G(\omega)$ and the $\alpha^2F(\omega)$ function for the higher-T_c junction. A decreasing $\alpha(\omega)$ with ω for small ω would result in a larger weighting[9] in the low-energy portion of $\alpha^2F(\omega)$. Nevertheless, the uncertainty in the sample quality used in the neutron work should be considered as well, since the agree-

TABLE I. A summary of the parameters from the proximity inversion analysis of two A15 Nb-Al junctions and one Nb_3Sn junction.

	Composition	T_c (K) (expt)	Δ (meV) (expt)	$\frac{2\Delta}{k_B T_c}$ (expt)	λ	μ^*	$\omega_{\log}^{b}$ (meV)	$\langle\omega\rangle^{b}$ (meV)	$\langle\omega^2\rangle^{b}$ $(meV)^2$	T_c (K)[c] (calc)	$\frac{2\Delta}{k_B T_c}$ (calc)	$\frac{2d_n}{\hbar v_F^*}$ $(meV)^{-1}$	$\frac{d_n}{l}$
A15 Nb-Al	21.5 at.% Al	14.0 ±0.2	2.15	3.56	1.2 ±0.05	0.13 ±0.01	11.2	13.3	226	11.7	3.8	0.0055	0.065
	22.8 at.% Al	16.4 ±0.1	3.15	4.45	1.7 ±0.05	0.15 ±0.02	9.5	11.4	181	15.1	4.3	0.006	0.055
A15 Nb-Sn	25.0 at.% Sn	17.7 ±0.1	3.25	4.26	1.8 ±0.15	0.16 ±0.03	10.8	13.1	226	16.7	4.25	0.0097	0.13

[a] $\lambda = 2\int d\omega\omega^{-1}\alpha^2F(\omega)$.

[b] $\omega_{\log} = \exp\left[\frac{2}{\lambda}\int d\omega\omega^{-1}\ln\omega\alpha^2F(\omega)\right]$.

[c] $T_c = \frac{\langle\omega\rangle}{1.2}\exp\left(\frac{-1.04(1+\lambda)}{\lambda-\mu^*(1+0.62\lambda)}\right)$, see Ref. 30.

[d] See Ref. 21.

ment between $G(\omega)$ and $\alpha^2F(\omega)$ is better with the lower-T_c sample.

IV. DISCUSSION AND CONCLUSION

A. Material diagnosis

The data and analysis presented in the previous section show it is possible to conduct tunneling experiments on the metastable A15 compound Nb_3Al and thereby to gain insight into the fundamental mechanisms giving rise to the high-T_c superconductivity. The two crucial factors in the success of this tunneling work are the reliable tunnel barrier formed by the oxidized amorphous silicon and the well-controlled thin-film synthesis of the material itself. The employment of Si barriers has made routine the fabrication of junctions with the desired characteristic of low leakage conductance. One can then attribute complicated current behavior or multiple gap structures observed in IV curves to the materials or phases in the base electrode, rather than to an imperfect oxide barrier.

The existence of structural inhomogeneities on either a macro- or a microscale has been recognized in many high-T_c A15 compounds, both in bulk samples and in films. Special deposition techniques, such as gaseous doping[31] or epitaxy[18] can lead to enhanced T_c's, but the thickness dependence of the enhancement has been difficult to determine. The enhancement due to the self-epitaxial growth employed here for the A15 Nb_3Al has been shown by the tunneling experiments to be maintained for about 165 Å for a deposition at 950 °C. Thus an explicit description of the progressive film growth is achievable by experiments with a series of junctions of a varying thickness in the base electrode. Carrying out a similar experiment on high-T_c Nb_3Ge thin films may shed light on the role of the gas (oxygen) stabilization.[32]

A satisfactory description of the tunneling data of Nb_3Al has been obtained by the proximity inversion analysis, as was done previously with Nb (Ref. 28) and Nb_3Sn.[29] For thermally oxidized Nb tunnel junctions, the existence of a thin proximity layer at the interface between Nb and the oxide barrier is related to the complicated suboxides of Nb metal.[33] Lacking a reliable quantitative surface analysis on the Nb_3Al films, the exact nature of the presumed thin layer of weakened superconductivity remains unclear. As mentioned earlier, an excess conduction current below the gap, about 2–5%, still exists even for the best made Nb_3Al tunnel junctions. In worse cases, a "knee-like structure above the gap is often found for junctions when the base material (Nb_3Al) is deposited at high temperatures ≥ 1000 °C. Taking a value of about 2×10^7 cm/sec for the renormalized Fermi velocity of Nb_3Al,[34] the thickness and the mean free

path of this proximity layer are estimated to be about $3 \sim 5$ and $50 \sim 90$ Å, respectively. It is important to be aware that these values of the fitting parameters are derived under the assumption of a zero Δ_n and are only approximates describing the interface between the Nb_3Al electrode and the oxide barrier. The occurrence of a degraded, normal-like material in the first few atomic layers below the surface appears quite reasonable, considering the T_c's of the high-T_c $A15$ class are highly sensitive to impurities, disorder, and compositional variation. It is interesting to note comparable values of the parameters $2d_n/\hbar v_F^*$ and d_n/l were used in the proximity inversion analysis for Nb_3Sn,[29] as listed in Table I. The proximity layers occurred in the cases of both Nb_3Sn and Nb_3Al could be of the same origin although some evidence of a Sn-rich surface in Nb_3Sn junctions has been suggested.[35] Advanced surface characterization techniques may help to determine the nature of the proximity layer.

B. Strong-coupling and high-T_c superconductivity of Nb_3Al

The tunneling data give ample evidence that high-T_c Nb_3Al is a rather strong-coupled superconductor. This result disagrees with the $G(\omega)$ function from the neutron work,[9] which is a representative of a weak- to medium-coupled superconductor. The value of the Debye temperature, about 300 K, which is slightly larger than that of Nb_3Sn, tends not to support the strong coupling either.[4,36] However, the specific-heat measurement of Willens *et al.*[4] obtained a $\Delta C/\gamma T_c$ of 3.5 by extrapolation for an ideally sharp transition at 18.8 K. Recently, Stewart *et al.*[36] remeasured the heat capacity of a bulk Nb_3Al of an improved quality and also suggested that Nb_3Al is possibly even slightly stronger coupled than Nb_3Sn. These results are quite consistent with our tunneling work considering that $2\Delta/k_BT_c$ of Nb_3Al should further increase above 4.4 for $T_c > 16.4$ K according to the trend shown in Fig. 5. Furthermore, $\Delta C/\gamma T_c$ can be estimated[37] from $2\Delta/k_BT_c$ and indeed agrees well with the value of 3.5.

It is found that the electron-phonon coupling strength is strongly enhanced as the composition approaches the $A15$ phase boundary of 24 at.% Al for Nb_3Al. Simple arguments based on the empirical formula by Kresin *et al.*[21] show that the occurrence of a mode-softening mechanism is necessary to account for the dramatic change in the coupling strength. Indeed such lattice softening is confirmed by the change in $\alpha^2F(\omega)$ at low ω in the two Nb-Al junctions of different coupling strength. Since these two sets of tunneling data were obtained by the same experimental techniques and analyzed by the same inversion procedure, the observed change should be meaningful. Recently Kimhi *et al.*[38] have shown that in crystalline Nb there is a relative enhancement of the low-frequency side lobe structures in $\alpha^2F(\omega)$ as the crystal structure becomes less ordered. Such behavior suggests that the pronounced soft modes observed in $\alpha^2F(\omega)$ of high-T_c Nb-Al could be related to the incipient instability derived from the Nb linear chains which are subject to substantial compression.[39] Furthermore, it has been found in some simple metal alloys, such as Pb-Bi, that a soft-mode mechanism results in the enhancement of λ and ultimately leads to structural instability and phase disproportionation.[40] This appears to correlate with the case of Nb_3Al as the composition approaches $A15$ phase boundary before disproportionating into the two phases.

One important question yet needs to be answered: what is the most dominant factor giving rise to the high T_c in Nb_3Al? In Table I, we have listed, for comparison, the physical parameters for Nb_3Sn obtained from tunneling analyzed by the proximity inversion method.[28] Note that λ and μ^* are comparable in Nb_3Al and Nb_3Sn; however, there is a significant reduction of about 20% in $\langle\omega^2\rangle$ and other frequency moments of Nb_3Al. Heat-capacity measurements[4,36] on bulk Nb_3Al samples show a rather low electronic of specific-heat coefficient γ, only about 60% of that of Nb_3Sn. Thus a larger $\langle I^2\rangle/\langle\omega^2\rangle$, partly resulting from the smaller $\langle\omega^2\rangle$, is required to compensate the lower electronic density of states at the Fermi level in order to obtain λ. By evaluating the band densities of states from the critical field measurements on Nb_3Al thin films, a more complete analysis of determining the high-T_c superconductivity from $N(0)$, $\langle I^2\rangle$, and $\langle\omega^2\rangle$ has been carried out and will be reported elsewhere.[34] From the present study we believe the important contribution of lattice softening to the high T_c in the metastable Nb_3Al has been well established rather than a large $N(0)$ conventionally used to explain the high T_c and normal-state properties of V_3Si and Nb_3Sn.

Furthermore, we find that $\langle\omega\rangle$'s change sensitively with composition or perhaps disorder. Such changes in $\langle\omega\rangle$'s have not previously been considered in modeling the rapid depression of T_c with disorder in $A15$ compounds.[41] For the stable $A15$ Nb_3Sn which is known to have a large $N(0)$, examining the trend of the increasing coupling strength of Nb_3Sn with the Sn composition as shown in Fig. 5 and the qualitative features in the corresponding $R(\omega)$'s of Nb_3Sn junctions[23] suggests that there is likely an enhanced weighting in $\alpha^2F(\omega)$ at low ω for the high T_c and strong-coupling Nb_3Sn. Although the existence of a large $N(0)$ in case of the more unstable Nb_3Ge has not been resolved, the strong-coupling nature was found[42] and some less systematic data[25] show the similar enhancement of the coupling strength with the increasing Ge concentration of the $A15$. It thus seems to be generally true that there is a marked lattice softening as a function of composition right near

the metalloid limit of stability in the Nb_3X high-T_c superconductors which must be of significance in contributing to the high T_c.

ACKNOWLEDGMENTS

We wish to thank Dr. M. R. Beasley, Dr. T. Claeson, Dr. R. H. Hammond, and Dr. J. M. Rowell for many helpful discussions during the course of this study. One of us (J.K.) is very grateful to D. F. Moore for his encouragement on initiating this work and his tutelage in the tunneling experiment. We also thank D. B. Kimhi, D. A. Rudman, and S. R. Ruggiero for their experimental assistance. This work supported by the Air Force Office of Scientific Research Contract No. F49620-78-C-0009.

*Also at Bell Laboratories, Murray Hill, N.J. 07974.

[1]M. Weger and I. B. Goldberg, Solid State Phys. 28, 1 (1973).

[2]D. F. Moore, R. B. Zubeck, J. M. Rowell, and M. R. Beasley, Phys. Rev. B 20, 2721 (1979).

[3]D. A. Rudman, R. E. Howard, D. F. Moore, R. B. Zubeck, and M. R. Beasley, IEEE Trans. Magn. 15, 582 (1979).

[4]R. H. Willens, T. H. Geballe, A. C. Gossard, J. P. Maita, A. Menth, G. W. Hull, Jr., and R. R. Soden, Solid State Commun. 7, 837 (1969).

[5]G. R. Stewart, L. R. Newkirk, and F. A. Valencia, Solid State Commun. 26, 417 (1978).

[6]C. C. Tsuei, S. von Molnar, and M. J. Coy, Phys. Rev. Lett. 41, 664 (1978).

[7]The Nb-Al phase diagram can be found in C. E. Lundin and A. S. Yamamoto, Trans. Am. Soc. Mech. Eng. 236, 863 (1966); V. N. Svechnikov, V. M. Pan, and V. I. Latzshev, Metallofizika. 32, 28 (1970); J. L. Jorda, R. Flükiger, A. Junod, and J. Muller, IEEE Trans. Magn. (in press).

[8]E. Ehrenfreund, A. C. Gossard, and J. H. Wernick, Phys. Rev. B 4, 2906 (1971).

[9]B. P. Schweiss, B. Renker, E. Schneider, and W. Reichardt, in *Superconductivity in d- and f-Band Metals,* edited by D. H. Douglas (Plenum, New York, 1976), p. 189.

[10]J. Kwo, R. H. Hammond, and T. H. Geballe, J. Appl. Phys. 51, 1726 (1980).

[11]R. H. Hammond, IEEE Trans. Magn. 11, 201 (1975); J. Vac. Sci. Technol. 15, 382 (1978).

[12]D. F. Moore, R. B. Zubeck, and M. R. Beasley, Bull. Am. Phys. Soc. 28, 289 (1977).

[13]L. Y. L. Shen, in *Superconductivity in d- and f-Band Metals,* edited by D. H. Douglas, AIP Conf. Proc. No. 4 (AIP, New York, 1972), p. 31.

[14]J. Bostock, V. Diadiuk, W. N. Chung, K. L. Lu, R. M. Rose, and M. L. A. Mac Vicar, Phys. Rev. Lett. 36, 603 (1976).

[15]D. A. Rudman and M. R. Beasley, Appl. Phys. Lett. 36, 1010 (1980).

[16]A. F. Hebard and J. R. Arthur, Bull. Am. Phys. Soc. 22, 374 (1977).

[17]J. T. C. Yeh and C. C. Tsuei, IEEE Trans. Magn. 15, 591 (1979).

[18]A. H. Dayem, T. H. Geballe, R. B. Zubeck, A. B. Hallak, and G. W. Hull, Jr., J. Phys. Chem. Solids 39, 529 (1978).

[19]W. L. McMillan, Phys. Rev. 175, 537 (1968).

[20]The composition of the A15 component of a two-phase sample is obtained by the extrapolation method according to the linear relation $\Delta T_c/\Delta C$ of 1.9 K/at.% Al in the single-phase A15 region. This method is described in detail in Ref. 10.

[21]V. Z. Kresin and V. P. Parkhomenko, Sov. Phys. Solid State 16, 2180 (1975) [Fiz. Tverd. Tela (Leningrad) 16, 3363 (1974)].

[22]S. Bermon (unpublished).
$N\exp(\omega)=(dI/dV)_s/(dI/dV)_n=(dV/dI)_n/(dV/dI)_s$,
$N_{\rm BCS}(\omega)=\omega/(\omega^2-\Delta^2)^{1/2}$.

[23]D. F. Moore, M. R. Beasley, and J. M. Rowell, J. Phys. (Paris) Colloq. 39, C8-1390 (1978).

[24]W. L. McMillan and J. M. Rowell, in *Superconductivity,* edited by R. D. Parks (Marcel-Dekker, New York, 1969), Vol. 1, p. 561.

[25]D. F. Moore, Ph.D. thesis (Stanford University, 1978) (unpublished).

[26]Gerald B. Arnold, Phys. Rev. B 18, 1076 (1978).

[27]E. L. Wolf, J. W. Osmon, John Sasadzinski, and Gerald B. Arnold, Solid State Commun. 31, 321 (1979).

[28]J. Bostock, M. L. A. MacVicar, Gerald B. Arnold, John Zasadzinski, and E. L. Wolf, in *Superconductivity in d- and f-Band Metals,* edited by H. Suhl and M. B. Maple (Academic, New York, 1980), p. 153.

[29]E. L. Wolf, John Zasadzinski, G. B. Arnold, D. F. Moore, J. M. Rowell, and M. R. Beasley, Phys. Rev. B 22, 1214 (1980).

[30]W. L. McMillan, Phys. Rev. 167, 331 (1968); P. B. Allen and R. C. Dynes, Phys. Rev. B 11, 1895 (1975). The T_c value calculated by the formula of the latter reference is about 1 K lower than that by the former reference.

[31]J. R. Gavaler, J. W. Miller, and B. R. Appleton, Appl. Phys. Lett. 28, 237 (1976); R. A. Sigsbee, *ibid.* 29, 211 (1976); A. B. Hallak, R. H. Hammond, and T. H. Geballe, *ibid.* 29, 314 (1976).

[32]J. R. Gavaler, M. Ashkin, A. I. Braginski, and A. T. Santhanan, Appl. Phys. Lett. 33, 359 (1978); B. Krevet, W. Schauer, and F. Wüchner, *ibid.* 36, 704 (1980).

[33]I. Lindau and W. E. Spicer, J. Appl. Phys. 45, 3720 (1974); M. Grundner and J. Halbritter, *ibid.* 51, 397 (1980).

[34]The ν_F^* value of Nb_3Al is obtained from the critical-field measurements. J. Kwo and T. P. Orlando and M. R. Beasley (unpublished).

[35]R. E. Howard, D. A. Rudman, and M. R. Beasley, Appl. Phys. Lett. 33, 671 (1978).

[36]G. R. Stewart and A. R. Sweedler (unpublished).

[37]$\Delta C/\gamma T_c=1.43\eta_{H_c}^2(T_c)$, $\eta_{H_c}(T_c)=1+(\pi T_c/\omega_0)^2\times(1.1\ln\omega_0/T_c+0.14)$. See Ref. 21.

[38]D. B. Kimhi and T. H. Geballe, Phys. Rev. Lett. 45, 1039 (1980).

[39]R. D. Burbank, R. C. Dynes, and J. M. Poate, J. Low Temp. Phys. 36, 573 (1979).

[40]R. C. Dynes and J. Rowell, Phys. Rev. B 11, 1884 (1975).

[41]L. R. Testardi and L. F. Mattheiss, Phys. Rev. Lett. 41, 1612 (1978).

[42]J. M. Rowell and P. H. Schmidt, Appl. Phys. Lett. 29, 622 (1976).